

A Little Higgs Model with Exact Dark Matter Parity

A. FREITAS¹, P. SCHWALLER², D. WYLER²

¹ *Department of Physics & Astronomy, University of Pittsburgh,
3941 O'Hara St, Pittsburgh, PA 15260, USA*

² *Institut für Theoretische Physik, Universität Zürich,
Winterthurerstrasse 190, CH-8057 Zürich, Switzerland*

Abstract

Based on a recent idea by Krohn and Yavin, we construct a little Higgs model with an internal parity that is not broken by anomalous Wess-Zumino-Witten terms. The model is a modification of the “minimal moose” models by Arkani-Hamed et al. and Cheng and Low. The new parity prevents large corrections to oblique electroweak parameters and leads to a viable dark matter candidate. It is shown how the complete Standard Model particle content, including quarks and leptons together with their Yukawa couplings, can be implemented. Successful electroweak symmetry breaking and consistency with electroweak precision constraints is achieved for natural parameters choices. A rich spectrum of new particles is predicted at the TeV scale, some of which have sizable production cross sections and striking decay signatures at the LHC.

1 Introduction

Little Higgs models are effective non-supersymmetric theories with a natural cutoff scale at about 10 TeV, where the Higgs scalar is a pseudo-Goldstone boson of a global symmetry, which is spontaneously broken at a scale $f \sim 1$ TeV. The symmetry breaking pattern protects the Higgs mass from quadratically divergent one-loop corrections, which are cancelled by new gauge bosons and fermions with masses near f . Therefore the hierarchy of scales can be realized without fine-tuning the parameters in the Higgs potential. A simple implementation of this mechanism is given by the “minimal moose” model of Ref. [1]. This model has two copies of the Standard Model (SM) gauge group, which are broken to the diagonal group at the scale f , reminiscent of chiral symmetry breaking in QCD.

However, tree-level mixing between the gauge bosons introduces large corrections to the oblique electroweak parameters for $f \sim 1$ TeV, unless the gauge couplings of the two gauge sectors are almost equal [2]. This equality of couplings can be explained by a discrete symmetry called T-parity [3, 4], under which the SM fields are T-even and the new TeV-scale particles are odd¹. As a result, all tree-level interactions between T-even and T-odd particles are forbidden, so that corrections to the electroweak precision observables occur only at one-loop level and thus are sufficiently small to allow values of f of 1 TeV and below. Furthermore, the lightest T-odd particle is stable and, if neutral, can be a good dark matter candidate.

Often it is assumed that the new physics entering near the scale of 10 TeV are some strong dynamics similar to technicolor theories². In this case, however, the fundamental theory can induce a Wess-Zumino-Witten (WZW) term [8], which is T-odd [9] if T-parity is implemented as in Ref. [4]. The breaking of T-parity by the WZW term, though suppressed by the large symmetry breaking scale, rules out the lightest T-odd particle as a dark matter candidate, since this particle would decay promptly into gauge bosons [10]. On the other hand, it was recently shown that a different construction of the parity in moose models leads to a parity-even WZW term [11]. The authors present a simple toy model that shows the relevant features.

In this article we adopt the idea of Ref. [11] for the “minimal moose” model in order to construct a fully realistic model which reproduces the Standard Model as a low-energy theory, admits electroweak symmetry breaking (EWSB), is consistent with electroweak precision constraints, and has a viable dark matter candidate. In the following section, the model and the implementation of the new X-parity is described explicitly. In section 3 the physical mass spectrum of the model is analyzed, and it is shown that successful electroweak symmetry breaking can be achieved. Finally, section 4 discusses electroweak precision constraints and gives a brief overview of the collider phenomenology, before the conclusions are presented in section 5.

¹A different discrete symmetry, which does not lead to a complete doubling of the SM particle content, has been proposed in Ref. [5, 6].

²An alternative approach involving a weakly coupled symmetry breaking sector can be found in Ref. [7].

2 The model

The model is based on a large $SU(3)^8 = [SU(3)_L \times SU(3)_R]^4$ global symmetry group that is spontaneously broken to the diagonal vector group $SU(3)_V^4$ at a scale f , giving rise to four sets of $SU(3)$ valued nonlinear sigma model fields

$$X_i = e^{2ix_i/f}, \quad i = 1, \dots, 4. \quad (1)$$

Under the global symmetry group they transform as $X_{1,3} \rightarrow L_{1,3}X_{1,3}R_{1,3}^\dagger$ and $X_{2,4} \rightarrow R_{2,4}X_{2,4}L_{2,4}^\dagger$. The axial components of the global symmetries shift the Goldstone fields, $x_i \rightarrow x_i + \epsilon_i$, thereby forbidding any nonderivative couplings for the Goldstone fields. In particular, as long as these symmetries are not explicitly broken, a mass term can't be generated for the Goldstone fields at any loop order.

Adding gauge and Yukawa interactions will in general break some of the global symmetries and therefore generate $\mathcal{O}(f)$ mass terms for the corresponding Goldstone bosons. The idea of collective symmetry breaking is to implement the required interactions in such a way that each interaction respects parts of the global symmetry and therefore keeps the corresponding Goldstone bosons massless. Only the simultaneous presence of different symmetry breaking interactions can then generate a mass for those Goldstone bosons. Since appropriate diagrams only appear at the two-loop level, the generated masses are suppressed by an additional loop factor and can be significantly below the scale f .

Our goal is to have at least one light electroweak doublet that we can identify with the SM Higgs boson. Under the SM gauge interactions, the Goldstone fields x_i decompose as follows

$$x_i = \begin{pmatrix} \phi_i + \eta_i/\sqrt{12} & h_i/2 \\ h_i^\dagger/2 & -\eta_i/\sqrt{3} \end{pmatrix}, \quad (2)$$

where $\phi_i = \phi_i^a \sigma^a/2$ are triplets under the $SU(2)$ gauge group, h_i are complex doublets, and η_i are real singlets. We further demand that the physical Higgs boson is even under the dark matter parity that acts as $x_1 \leftrightarrow x_2$ and $x_3 \leftrightarrow x_4$ on the Goldstone fields. This leaves us with two candidates for the SM Higgs doublets,

$$h_a \equiv \frac{1}{\sqrt{2}}(h_3 + h_4), \quad h_b \equiv \frac{1}{\sqrt{2}}(h_1 + h_2). \quad (3)$$

The physical Higgs field will later be identified as h_a and is protected by the global symmetries $SU(3)_{L,a} = SU(3)_{L,3} \times SU(3)_{L,4}/SU(3)_{DL}$ and $SU(3)_{R,a} = SU(3)_{R,3} \times SU(3)_{R,4}/SU(3)_{DR}$, where $SU(3)_{Di}$ denotes the diagonal subgroups of these product groups. As long as no single interaction breaks both $SU(3)_{L,a}$ and $SU(3)_{R,a}$ at the same time, the mass of the Higgs will be sufficiently small.

For models based on the symmetry structure used here, possibilities to introduce interactions that preserve enough global symmetries are discussed in [1]. We found that we could adopt their rules to introduce scalar self-interactions as well as gauge interactions, but that some modifications are required in the Yukawa sector in order to maintain the parity symmetry. In particular partners for the standard model fermions must be introduced so that the dark matter parity can be implemented in a linear way.

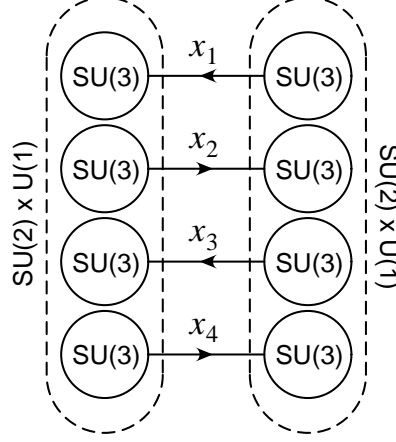


Figure 1: Illustration of the global and gauge symmetry structure of the model.

2.1 Scalar and gauge sector

The global symmetry structure of the model is depicted in Fig. 1. On each site, a $SU(2) \times U(1)$ subgroup is gauged, with equal strength for both sites. The gauge group generators are given by

$$Q_{L,R}^a = \begin{pmatrix} \sigma^a/2 & 0 \\ 0 & 0 \end{pmatrix}, \quad Y_{L,R} = \frac{1}{\sqrt{12}} \begin{pmatrix} 1 & 0 \\ 0 & -2 \end{pmatrix}, \quad (4)$$

written in terms of 2×2 and 1×1 blocks. Here σ^a denote the Pauli matrices. The kinetic term of the sigma fields reads

$$\mathcal{L}_G = \frac{f^2}{4} \sum_{i=1}^4 \text{tr}[(D_\mu X_i)(D^\mu X_i)^\dagger], \quad \text{with} \quad \begin{aligned} D_\mu X_{1,3} &= \partial_\mu X_{1,3} - iA_{L\mu}X_{1,3} + iX_{1,3}A_{R\mu}, \\ D_\mu X_{2,4} &= \partial_\mu X_{2,4} - iA_{R\mu}X_{2,4} + iX_{2,4}A_{L\mu}, \end{aligned} \quad (5)$$

$$\text{and} \quad A_{L\mu} \equiv g_L W_{L\mu}^a Q_L^a + g'_L y_{LX} B_{L\mu} Y_L, \quad (6)$$

$$A_{R\mu} \equiv g_R W_{R\mu}^a Q_R^a + g'_R y_{RX} B_{R\mu} Y_R, \quad (7)$$

where the gauge couplings at the two sites are chosen to be equal, $g_L = g_R = \sqrt{2}g$ and $g'_L = g'_R = \sqrt{2}g'$, and g, g' are the SM gauge couplings. Furthermore, $y_{LX, RX}$ denote the $U(1)$ charges of the fields X_i . The choice $y_{LX} = y_{RX} = 1/\sqrt{3}$ ensures the correct values for the Higgs doublet hypercharge and Weinberg angle. Note that the definition (5) of the covariant derivatives corresponds to assigning opposite directions for the link fields 1,3 and 2,4, which is important for the definition of the X-parity below.

Each gauge interaction separately only break either $SU(3)_{L,a}$ or $SU(3)_{R,a}$ and therefore respects collective symmetry breaking. Actually since the gauge interactions are either on the left or on the right side of the moose diagram, no large mass is generated for any of the Goldstone fields from these interactions.

The kinetic term (5) has a \mathbb{Z}_2 symmetry, called X-parity, defined by

$$\text{X-parity:} \quad A_L \leftrightarrow A_R, \quad X_1 \leftrightarrow X_2, \quad X_3 \leftrightarrow X_4. \quad (8)$$

This definition is a straightforward generalization of the parity of the two-link model in Ref. [11]. Under this parity, the WZW terms [8] for the four link fields transform as

$$\Gamma_{\text{WZW}}(x_1, A_L, A_R) \leftrightarrow \Gamma_{\text{WZW}}(x_2, A_R, A_L), \quad \Gamma_{\text{WZW}}(x_3, A_L, A_R) \leftrightarrow \Gamma_{\text{WZW}}(x_4, A_R, A_L), \quad (9)$$

so that the combined term

$$\mathcal{L}_{\text{WZW}} = \Gamma_{\text{WZW}}(x_1, A_L, A_R) + \Gamma_{\text{WZW}}(x_2, A_R, A_L) + \Gamma_{\text{WZW}}(x_3, A_L, A_R) + \Gamma_{\text{WZW}}(x_4, A_R, A_L) \quad (10)$$

remains invariant. As a result, X-parity is an exact symmetry of the model and the lightest X-odd particle is stable.

In addition to the X-parity in eq. (8) a second \mathbb{Z}_2 symmetry, called T-parity, is imposed, under which

$$\text{T-parity:} \quad A_L \leftrightarrow A_R, \quad X_i \rightarrow \Omega X_i^\dagger \Omega, \quad (11)$$

where $\Omega \equiv \text{diag}(1, 1, -1)$. Our T-parity is identical to the original version in Ref. [4], and it ensures that the triplet and singlet scalar do not receive any vacuum expectation values. In our implementation, T-parity is respected by the model at the classical level, but broken by \mathcal{L}_{WZW} . However, since the stability of the dark matter candidate is already guaranteed by X-parity (8), this does not lead to any problems.

In the gauge sector, the X-odd linear combinations of gauge bosons,

$$W_H^a = \frac{1}{\sqrt{2}}(W_L^a - W_R^a), \quad B_H = \frac{1}{\sqrt{2}}(B_L - B_R), \quad (12)$$

acquire masses of order f from the kinetic term (5), while the X-even combinations

$$W^a = \frac{1}{\sqrt{2}}(W_L^a + W_R^a), \quad B = \frac{1}{\sqrt{2}}(B_L + B_R), \quad (13)$$

remain massless before EWSB and are identified with the SM gauge bosons. The scalar fields form the following X-even and X-odd combinations:

$$w = \frac{1}{2}(x_1 - x_2 + x_3 - x_4) \quad x = \frac{1}{2}(-x_1 + x_2 + x_3 - x_4) \quad (\text{X-odd}), \quad (14)$$

$$y = \frac{1}{2}(-x_1 - x_2 + x_3 + x_4) \quad z = \frac{1}{2}(x_1 + x_2 + x_3 + x_4) \quad (\text{X-even}). \quad (15)$$

The triplet ϕ_w and the singlet η_w are eaten to form the longitudinal components of W_H^a and B_H .

A large Higgs quartic coupling, required for electroweak symmetry breaking, is generated by the following X-invariant plaquette operator:

$$\mathcal{L}_P = \frac{\kappa}{8} f^4 \text{tr} \left[X_1 X_3^\dagger X_2^\dagger X_4 + X_2 X_4^\dagger X_1^\dagger X_3 \right] + \text{h.c.} \quad (16)$$

This operator contains an explicit $\mathcal{O}(f)$ mass term for the scalar fields in x , but preserves enough global symmetries so it does not generate large masses for any other Goldstone bosons at the one loop level, in particular not for h_a, h_b .

Successful electroweak symmetry also requires the introduction of a second plaquette term [1], which breaks a different subset of the global symmetry:

$$\mathcal{L}'_p = \frac{\epsilon}{8} f^4 \text{tr} \left(T_8 X_1 X_3^\dagger X_2^\dagger X_4 + T_8 X_2 X_4^\dagger X_1^\dagger X_3 + X_1 X_3^\dagger T_8 X_2^\dagger X_4 + X_2 X_4^\dagger T_8 X_1^\dagger X_3 \right) + \text{h.c.} \quad (17)$$

where $T_8 = \text{diag}(1, 1, -2)/\sqrt{12}$, and ϵ is a complex constant. As explained in Ref. [1], eq. (17) can be generated radiatively by two-loop diagrams involving the top quark, and therefore it is natural to assume that $|\epsilon| \sim |\kappa|/10$. We can assume ϵ to be purely imaginary, since the real part only gives small corrections to the scalar potential.

2.2 Fermion sector

For the construction of the kinetic and Yukawa terms of the fermions, several conditions need to be considered. First, one has to make sure that these terms do not break too many of the global symmetries, so that the mass of the little Higgs doublet remains protected from quadratic corrections. Secondly, the minimal construction using only X-even fermions [4] leads to unsuppressed four-fermion operators at one-loop level, thus forcing the scale f be about 10 TeV or larger [12]. The second problem can be solved by introducing “mirror” fermions [12], *i. e.* two sets of fermions that are partners under X-parity. Our implementation closely resembles the setup in the appendix of Ref. [13].

For each SM flavor two doublets of left-handed fermions are introduced, located at the two sites of the moose diagram. With the exception of the top quark, they are embedded into incomplete representations of SU(3) as follows

$$Q_a = (d_a, u_a, 0)^\top, \quad Q_b = (d_b, u_b, 0)^\top. \quad (18)$$

Under the global SU(3)_L × SU(3)_R group they transform as $Q_a \rightarrow L_i Q_a$ and $Q_b \rightarrow R_i Q_b$, while X- and T-parity interchange the two fields, $Q_a \leftrightarrow Q_b$.

Since (18) are incomplete multiplets, their interaction terms break the global symmetries that protect the Higgs mass and lead to quadratically divergent contributions from one-loop diagrams involving the Yukawa couplings. For the first two generations this is not a problem since the Yukawa couplings are very small, but for the third generation we need to introduce complete multiplets

$$Q_{3a} = (d_{3a}, u_{3a}, U_a)^\top, \quad Q_{3b} = (d_{3b}, u_{3b}, U_b)^\top. \quad (19)$$

Here the additional singlets $U_{a,b}$ cancel the quadratically divergent Higgs mass contributions induced by the large top Yukawa coupling.

The X- and T-invariant fermion kinetic terms have the standard form

$$\mathcal{L}_F = i\bar{Q}_a \bar{\sigma}^\mu D_\mu^a Q_a + i\bar{Q}_b \bar{\sigma}^\mu D_\mu^b Q_b, \quad \text{with} \quad D_\mu^a = \partial_\mu + ig_L W_{L\mu}^a (Q_L^a)^\top - ig_L' y_{LQ} B_{L\mu}, \quad (20)$$

$$D_\mu^b = \partial_\mu + ig_R W_{R\mu}^a (Q_R^a)^\top - ig_R' y_{RQ} B_{R\mu},$$

where $\bar{\sigma}^\mu \equiv (1, -\vec{\sigma})$, and y_{LQ} and y_{RQ} are diagonal matrices composed of the U(1) charges in Table 1. The SM fermions emerge from the X-even linear combination $Q = \frac{1}{\sqrt{2}}(Q_a + Q_b)$.

To give mass to the X-odd combination $Q_H = \frac{1}{\sqrt{2}}(Q_a - Q_b)$, we need to introduce conjugate Dirac partners

$$Q_c^c = (d_c^c, u_c^c, 0)^\top, \quad Q_{3c}^c = (d_{3c}^c, u_{3c}^c, U_c^c)^\top, \quad (21)$$

Under $SU(3)_L \times SU(3)_R$ they transform as $Q_c^c \rightarrow U_i Q_c^c$, where U_i ($i = 1, \dots, 4$) belongs to the unbroken diagonal subgroup of $SU(3)_L \times SU(3)_R$ and is a non-linear function of L_i and R_i . Furthermore, the effect of X- and T-parity is defined as $Q_c^c \rightarrow -\Omega Q_c^c$. Then a X- and T-invariant mass term for the X-odd fermions is given by

$$\mathcal{L}_M = -\frac{\lambda_c}{\sqrt{2}} f \left(Q_a \xi_1 Q_c^c - Q_b \Omega \xi_1^\dagger Q_c^c - Q_b \xi_2 \Omega Q_c^c + Q_a \Omega \xi_2^\dagger \Omega Q_c^c \right) + \text{h.c.}, \quad (22)$$

where $\xi_i = e^{ix_i/f}$. Under global $SU(3)_L \times SU(3)_R$ rotations ξ_i transforms as $\xi_i \rightarrow L_i \xi_i U_i^\dagger = U_i \xi_i R_i^\dagger$ for $i = 1, 3$ and analogous for $i = 2, 4$, so that eq. (22) is evidently gauge invariant. In general, λ_c is a 3×3 matrix in flavor space. Since it can contribute to flavor-changing neutral currents (FCNCs) at one-loop level, it is constrained by data on heavy-flavor decays and oscillations. Such effects are studied for example in [14] for the case of the littlest Higgs model with T-parity. For the analyses in section 3 and 4 we assume a flavor diagonal λ_c for simplicity.

Since the Q_c^c transform non-linearly, one must make use of the ξ_i fields to construct a gauge- and X- and T-invariant kinetic term. Following the formalism of Callan, Coleman, Wess, and Zumino [15], it can be written as

$$\mathcal{L}_c = i \bar{Q}_c^c \bar{\sigma}^\mu \left(\partial_\mu + \frac{1}{4} (\xi_1^\dagger D_\mu \xi_1 + \xi_1 D_\mu \xi_1^\dagger + \xi_2^\dagger D_\mu \xi_2 + \xi_2 D_\mu \xi_2^\dagger) - ig' (y_{Q_c} + \frac{1}{\sqrt{3}} Y_V) B_\mu \right) Q_c^c, \quad (23)$$

where

$$\xi_i^\dagger D_\mu \xi_i = \xi_i^\dagger (\partial_\mu + ig W^a Q_V^a + ig W_H^a Q_A^a + ig' \frac{1}{\sqrt{3}} B Y_V + ig' \frac{1}{\sqrt{3}} B_H Y_A) \xi_i, \quad (24)$$

$$\xi_i D_\mu \xi_i^\dagger = \xi_i (\partial_\mu + ig W^a Q_V^a - ig W_H^a Q_A^a + ig' \frac{1}{\sqrt{3}} B Y_V - ig' \frac{1}{\sqrt{3}} B_H Y_A) \xi_i^\dagger, \quad (25)$$

and Q_V^a, Y_V and Q_A^a, Y_A are the unbroken and broken gauge generators, respectively. Both equations (22) and (23) do not involve the x_3 and x_4 Goldstone fields and therefore do not break the global symmetries that protect the Higgs mass. They do however generate masses for some of the other Goldstone bosons that will be explicitly calculated in section 3.2.

Now Yukawa couplings can be constructed for the X-even massless combinations of the fermions. For the up-type quarks of the first two generations they read

$$\mathcal{L}_u = -\lambda_u f Q_a (X_3 + \Omega X_4^\dagger \Omega) \begin{pmatrix} 0 \\ 0 \\ u^c \end{pmatrix} - \lambda_u f Q_b (\Omega X_3^\dagger \Omega + X_4) \begin{pmatrix} 0 \\ 0 \\ u^c \end{pmatrix} + \text{h.c.}, \quad (26)$$

where u^c are the right-handed quarks (one for each flavor), which are X- and T-even. As already mentioned above, the presence of incomplete multiplets in the Yukawa couplings

leads to quadratically divergent contribution to the Higgs mass. Therefore the top Yukawa coupling has a slightly different form [13],

$$\mathcal{L}_t = -\lambda f Q_{3a}(X_3 + \Omega X_4^\dagger \Omega) \begin{pmatrix} 0 \\ 0 \\ U_b^c \end{pmatrix} - \lambda f Q_{3b}(\Omega X_3^\dagger \Omega + X_4) \begin{pmatrix} 0 \\ 0 \\ U_a^c \end{pmatrix} + \text{h.c.} \quad (27)$$

Here the two singlets U_a^c and U_b^c transform under X- and T-parity as $U_a^c \leftrightarrow U_b^c$. Their X-even combination $U_a^c + U_b^c$ emerges in the right-handed top quark, while the X-odd combination $U_a^c - U_b^c$ forms the right-handed partner of the X-odd $U_a - U_b$. In addition there are one more X-even and X-odd fermion in the top sector, which receive masses from eq. (22). This will be explained in more detail in section 3.1.

The use of complete multiplets Q_{3a} , Q_{3b} in (27) makes sure that each term preserves one of the global SU(3) symmetries that protect the Higgs mass.

Finally, the down-type Yukawa couplings are given by

$$\mathcal{L}_d = -\lambda_d f \tilde{Q}_a(X_3 + \Omega X_4^\dagger \Omega)^* \begin{pmatrix} 0 \\ 0 \\ d^c \end{pmatrix} - \lambda_d f \tilde{Q}_b(\Omega X_3^\dagger \Omega + X_4)^* \begin{pmatrix} 0 \\ 0 \\ d^c \end{pmatrix} + \text{h.c.}, \quad (28)$$

where

$$\tilde{Q}_{a,b} = -2iT_2 Q_{a,b} = (-u_{a,b}, d_{a,b}, 0)^\top, \quad T_2 = \begin{pmatrix} \sigma^2/2 & 0 \\ 0 & 0 \end{pmatrix}. \quad (29)$$

The lepton Yukawa interactions are defined similarly. In contrast to the up-type Yukawa couplings, the all three generations of down-type fermions generate quadratically divergent contributions to the Higgs doublet masses from eq. (28), which is permissible since the bottom Yukawa coupling is much smaller than the top Yukawa coupling. The kinetic term for the singlet conjugate fields $\psi^c \equiv u^c, d^c, U_a^c, U_b^c$ simply reads

$$\mathcal{L}_R = i\bar{\psi}^c \sigma^\mu (\partial_\mu - ig' y_{\psi^c} B_\mu) \psi^c = i\bar{\psi}^c \sigma^\mu (\partial_\mu - i\sqrt{2}g'(y_{L\psi^c} B_{L\mu} + y_{R\psi^c} B_{R\mu})) \psi^c, \quad (30)$$

where $\sigma^\mu \equiv (1, \vec{\sigma})$ and $y_{\psi^c} = 2y_{L\psi^c} = 2y_{R\psi^c}$ is the fermion hypercharge.

Table 1 summarizes the fermion contained in the model and their transformation properties. Note that the model is non-renormalizable and considered to be a low-energy effective theory of some fundamental dynamics associated with the UV cutoff scale $\Lambda \sim 10 f \sim 10 \text{ TeV}$. This UV completion could, but does not need to, consist of some strongly coupled gauge interaction, which breaks the global symmetry through the formation of a fermion condensate, similar to technicolor.

	SU(2) _L	SU(2) _R	U(1) _L	U(1) _R	X	T
q_a	2	1	$\frac{1}{12}$	$\frac{1}{12}$	q_b	q_b
U_a	1	1	$\frac{7}{12}$	$\frac{1}{12}$	U_b	U_b
q_b	1	2	$\frac{1}{12}$	$\frac{1}{12}$	q_a	q_a
U_b	1	1	$\frac{1}{12}$	$\frac{7}{12}$	U_a	U_a
Q_c^c	nonlinear				$-\Omega Q_c^c$	$-\Omega Q_c^c$
d^c	1	1	$\frac{1}{6}$	$\frac{1}{6}$	d^c	d^c
u^c	1	1	$-\frac{1}{3}$	$-\frac{1}{3}$	u^c	u^c
U_a^c	1	1	$-\frac{7}{12}$	$-\frac{1}{12}$	U_b^c	U_b^c
U_b^c	1	1	$-\frac{1}{12}$	$-\frac{7}{12}$	U_a^c	U_a^c

Table 1: Quantum numbers of the fermion multiplets under the $[\text{SU}(2) \times \text{U}(1)]^2$ gauge symmetry, and their transformation properties under X and T . The physical $\text{U}(1)_Y$ hypercharge is the sum of both $\text{U}(1)_1 + \text{U}(1)_2$ charges. There is some freedom in the assignment of $\text{U}(1)_1$ and $\text{U}(1)_2$ charges to $U_a^{(c)}$, $U_b^{(c)}$. Here the conventions of [13] have been adapted.

3 Mass spectrum

3.1 Top quark sector

Expanding the Yukawa couplings (22) and (27) in the top quark sector in powers of $1/f$ yields

$$\begin{aligned}
\mathcal{L}_t = & -\sqrt{2}\lambda_c f(u_{3a} - u_{3b})u_{3c}^c - \sqrt{2}\lambda_c f(U_a + U_b)U_c^c - 2\lambda f(U_a U_b^c + U_b U_a^c) \\
& - \lambda(q_{3a}(h_y + h_z)U_b^c + q_{3b}(h_y + h_z)U_a^c) \\
& + \frac{1}{2\sqrt{2}}\lambda_c [(q_{3a} + q_{3b})(h_y - h_z)U_c^c + (U_a - U_b)(h_y^\dagger - h_z^\dagger)q_c^c] + \dots + \text{h.c.}, \quad (31)
\end{aligned}$$

where $q_{3a} = (d_{3a}, u_{3a})^\top$, $q_{3b} = (d_{3b}, u_{3b})^\top$, and the dots indicate $\mathcal{O}(f^{-1})$ terms and $\mathcal{O}(f^0)$ terms that do not involve Higgs doublets. With suitable phase redefinitions of the fields, both λ and λ_c can be chosen to be real³. Introducing the X-even and -odd combinations

$$U_\pm \equiv \frac{1}{\sqrt{2}}(U_a \pm U_b), \quad U_\pm^c \equiv \frac{1}{\sqrt{2}}(U_a^c \pm U_b^c), \quad (32)$$

$$q_{3\pm} \equiv \frac{1}{\sqrt{2}}(q_{3a} \pm q_{3b}), \quad u_{3\pm} \equiv \frac{1}{\sqrt{2}}(u_{3a} \pm u_{3b}), \quad (33)$$

one obtains

$$\begin{aligned}
\mathcal{L}_t = & -2\lambda_c f u_{3-} u_{3c}^c - 2\lambda_c f U_+ U_c^c - 2\lambda f (U_+ U_+^c + U_- U_-^c) \\
& - \lambda(q_{3+}(h_y + h_z)U_+^c + q_{3-}(h_y + h_z)U_-^c) + \frac{1}{2}\lambda_c q_{3+}(h_y - h_z)U_c^c + \text{h.c.} \quad (34)
\end{aligned}$$

³A relative factor i between the second line of (31) and (27) has been absorbed by this same procedure.

Neglecting contributions of order v^2/f^2 , the X-odd mass eigenstates in the top sector, written in terms of left- and right-handed components, are

$$(T_H, T_H^c) \equiv (u_{3-}, u_{3c}^c), \quad (T', T'^c) \equiv (U_-, U_-^c), \quad (35)$$

with masses $2\lambda_c f$ and $2\lambda f$, respectively. In the X-even top sector, the following Dirac fermions are formed:

$$(T, T^c) \equiv \left(U_+, \frac{\lambda_c U_+^c + \lambda U_+^c}{\sqrt{\lambda^2 + \lambda_c^2}} \right), \quad (t, t^c) \equiv \left(u_{3+}, \frac{\lambda_c U_+^c - \lambda U_+^c}{\sqrt{\lambda^2 + \lambda_c^2}} \right). \quad (36)$$

The T obtains a mass $m_T = 2\sqrt{\lambda^2 + \lambda_c^2}f$, while the SM-like top quark t remains massless before EWSB and has a Yukawa coupling given by

$$- \lambda_t q_3 h t^c + \text{h.c.}, \quad \lambda_t = \frac{\sqrt{2} \lambda \lambda_c}{\sqrt{\lambda^2 + \lambda_c^2}}. \quad (37)$$

Note that the X-odd top partner T' is responsible for the cancellation of the quadratically divergent contribution to the Higgs mass. Therefore the X-even T as well as the X-odd T_H can be given masses of several TeV by increasing λ_c , thus effectively decoupling them from the remaining fermion masses can be found in table 2.

Once electroweak symmetry is broken mixing of the top quark with the T quark is reintroduced. The resulting mass matrix can be diagonalized by redefining the t and T quark as follows:

$$t \rightarrow c_L t - s_L T, \quad T \rightarrow c_L T + s_L t, \quad (38)$$

$$t^c \rightarrow c_R t^c - s_R T^c, \quad T^c \rightarrow c_R T^c + s_R t^c, \quad (39)$$

where $s_L \equiv \sin \alpha_L$, $c_L \equiv \cos \alpha_L$ are the sine and cosine of the left-handed mixing angle and similarly for s_R , c_R . To leading order in an expansion in (v/f) , these mixing angles are given by

$$\sin \alpha_L \approx \alpha_L = \frac{\lambda}{\lambda_c} \frac{m_t}{m_T} + \mathcal{O}\left(\frac{m_t^2}{m_T^2}\right), \quad (40)$$

$$\sin \alpha_R \approx \alpha_R = 0 + \mathcal{O}\left(\frac{m_t^2}{m_T^2}\right), \quad (41)$$

while the mass eigenvalues remain unperturbed at this order.

3.2 Scalar masses

Since the non-linear sigma model breaks the complete symmetry down to its diagonal vector group, the X-odd SU(2) and U(1) gauge bosons, which are associated with the broken generators, become massive by eating the triplet ϕ_w and singlet η_w in the scalar w multiplet, respectively. The other scalars are pseudo-Goldstone bosons that receive masses from all

interactions that explicitly break some of the global symmetries. The only tree-level mass terms for the scalars stem from the plaquette operators (16) and (17), which lead to a mass $M_p^2 = 4\kappa f^2$ for all fields in the x multiplet, and additional $\mathcal{O}(\epsilon f^2)$ contributions to all doublet fields. However, at one- and two-loop level, scalar mass terms are generated from various other Lagrangian.

One-loop corrections from the mirror fermion mass term (22) induce a quadratically divergent mass for the linear combination $x_1 + x_2 = -(y - z)$, of order $\mathcal{O}[\lambda_c^2 \Lambda^2 / (16\pi^2)] \sim \mathcal{O}(\lambda_c^2 f^2)$. Similarly, the top Yukawa coupling (27) generates quadratically divergent one-loop mass terms, of order $\mathcal{O}(\lambda^2 f^2)$ for the doublets in $x_3 - x_4 = x + w$ and singlets in $x_3 + x_4 = y + z$. On the other hand, the kinetic term (23) leads to two-loop mass terms that have quartic divergences [4]. As a result, the scalar doublets in $x_1^2 + x_2^2 = \frac{1}{2}(w - x)^2 + \frac{1}{2}(y - z)^2$ pick up masses of order $\mathcal{O}[g^2 / (16\pi^2)^2 \times \Lambda^4 / f^2] \sim \mathcal{O}(g^2 f^2)$.

The remaining doublet and triplet linear combinations $h_y + h_z$ and $\phi_y + \phi_z$ are protected from quadratically divergent one-loop mass terms. However, all scalar fields obtain logarithmic one-loop contributions and quadratically divergent two-loop contributions from the gauge kinetic terms and the plaquette operator. Furthermore, the doublet $h_y + h_z$ receives a logarithmic one-loop mass term from the top Yukawa coupling. These mass contributions are parametrically of the order of the electroweak scale $v \sim f / (16\pi^2)$. The X-even doublet $h_y + h_z$ will become the dominant component of the light Higgs boson, which is responsible for electroweak symmetry breaking.

Including all the aforementioned contributions, the scalar mass terms are given by

$$\begin{aligned} \mathcal{L}_{\text{mass,scal}} = & -\frac{1}{2}[(M_p^2 + m_{g,S}^2 + m_{p,S}^2)\eta_x^2 + (M_t^2 + m_{g,S}^2 + m_{p,S}^2)(\eta_y^2 + \eta_z^2) + M_y^2(\eta_y - \eta_z)^2] \\ & -\frac{1}{2}[(M_p^2 + m_{g,T}^2 + m_{p,T}^2)|\phi_x|^2 + (m_{g,T}^2 + m_{p,T}^2)(|\phi_y|^2 + |\phi_z|^2) + \frac{3}{2}M_y^2|\phi_y - \phi_z|^2] \\ & -\frac{1}{2}[M_p^2|h_x|^2 + (M_t^2 + m_{g,D}^2 + m_{p,D}^2)(|h_x|^2 + |h_w|^2) + (M_{kin}^2 + M_y^2)|h_w - h_x|^2 \\ & + (M_{kin}^2 + M_y^2)|h_y - h_z|^2 + m_t^2|h_y + h_z|^2 + (m_{g,D}^2 + m_{p,D}^2)(|h_y|^2 + |h_z|^2) \\ & + i m_\epsilon^2(h_w^\dagger h_x - h_x^\dagger h_w + h_z^\dagger h_y - h_y^\dagger h_z)], \end{aligned} \quad (42)$$

where the singlet, triplet, and doublet mass terms are shown in the first, second, and remaining lines, respectively. The mass parameters are summarized in the following list:

$M_p^2 \equiv 4\kappa f^2$	plaquette mass
$m_\epsilon^2 \equiv \frac{\sqrt{3}}{2}f^2\text{Im}(\epsilon)$	ϵ -plaquette term from (17)
$M_{kin}^2 \equiv c_k g^2 f^2$	2-loop mass from (23)
$M_y^2 \equiv c_y \lambda_c^2 f^2$	1-loop mass from (22)
$m_{g,X}^2 \equiv c_{g,X} g^4 f^2 / (4\pi)^2 \log(g^2 f^2 / \Lambda^2)$	gauge-loop mass, log part
$M_t^2 \equiv c_T \lambda^2 f^2$	top loop from (27), quadratic divergent part
$m_{t,D}^2 \equiv c_t M_{T'}^2 / (4\pi)^2 \log(M_{T'}^2 / m_t^2)$	top loop from (27), log part
$m_{p,X}^2 \equiv c_{p,X} \kappa^2 f^2 / (4\pi)^2 \log(\kappa f^2 / \Lambda^2)$	plaquette-loop mass, log part

Here the $\mathcal{O}(f)$ terms are written in capital letters, while lower case is used for the lighter mass terms. m_t and $M_{T'}$ denote the top quark mass and the mass of the T' quark. The latter cancels the quadratic divergences in the top loop contribution to the Higgs mass. The c_i are $\mathcal{O}(1)$ coefficients, which, except for c_t , depend on unknown details of the UV completion. However, it is possible to determine the *relative* contributions of the gauge loops to the singlets, doublets, and triplets, which are given by $c_{g,S} = 0$ (since the singlets commute with all gauge generators), $c_{g,T} \sim 1/8$, and $c_{g,D} \sim \frac{3}{64}[1 + (g'/g)^4]$.

The doublet h_w does not get eaten and remains in the physical spectrum. It mixes with the other X-odd doublet h_x to form two mass eigenstates h_{H1} and h_{H2} with $\mathcal{O}(f)$ masses. λ_c can be relatively large, leading to a rather large splitting between the two masses, and to a large mixing. In the limit of large λ_c , the X-odd doublet masses are approximately given by $M_{H1}^2 \approx M_t^2 + M_p^2/2$ and $M_{H2}^2 \approx M_{H1}^2 + 2M_y^2 + 2M_{kin}^2$.

3.3 Electroweak symmetry breaking

The plaquette interactions (16) generate quartic couplings for the X-even scalars, which can be written as

$$- \kappa \text{tr}[y, z]^2. \quad (43)$$

Additional quartic interactions emerge from the second plaquette term (17) and from loop corrections but will be neglected at this point.

To further analyse the Higgs potential, it is useful to switch back to the basis (3) using

$$h_a = \frac{1}{\sqrt{2}}(h_y + h_z), \quad h_b = \frac{1}{\sqrt{2}}(h_y - h_z). \quad (44)$$

In this basis, the quartic potential for the X-even doublets reads

$$V_4 = \frac{\kappa}{8} \left[(h_a^\dagger h_a)(h_b^\dagger h_b) + (h_a^\dagger h_b)(h_b^\dagger h_a) - (h_a^\dagger h_b)^2 - (h_b^\dagger h_a)^2 \right], \quad (45)$$

while the quadratic potential, taken from eq. (42), is given by

$$V_2 = \frac{1}{2} \left[m_a^2 |h_a|^2 + m_b^2 |h_b|^2 + (m_{ab}^2 h_a^\dagger h_b + \text{h.c.}) \right], \quad (46)$$

with the mass parameters

$$m_a^2 = 2m_t^2 + m_{g,D}^2 + m_{p,D}^2, \quad (47)$$

$$m_b^2 = 2M_{kin}^2 + 2M_y^2 + m_{g,D}^2 + m_{p,D}^2, \quad (48)$$

$$m_{ab}^2 = -im_\epsilon^2. \quad (49)$$

As evident from these equations, electroweak symmetry breaking is described in this model by an effective Two-Higgs-Doublet model (2HDM). The conditions for successful symmetry breaking are

$$m_{g,D}^2 > -2m_t^2, \quad m_\epsilon^4 > (2M_y^2 + 2M_{kin}^2 + m_{g,D}^2 + m_{p,D}^2)(2m_t^2 + m_{g,D}^2 + m_{p,D}^2). \quad (50)$$

Since $m_{g,D}^2$ and m_t^2 are of the same order of magnitude and m_t^2 is negative, these conditions can be satisfied naturally. Without the m_e term, the Higgs potential would have an unsta-
bilized flat direction, and electroweak symmetry would not be broken to the SM vacuum.

The potential is then minimized by the vacuum expectation values

$$\langle h_a \rangle = (0, v \cos \beta)^\top \quad \langle h_b \rangle = (0, i v \sin \beta)^\top, \quad (51)$$

with

$$\tan^2 \beta = m_a^2/m_b^2 = \mathcal{O}(m^2/M^2), \quad (52)$$

where M denotes the $\mathcal{O}(f)$ masses in the scalar potential, while m represents any of the suppressed mass terms. We have checked numerically that for reasonable choices of the mass parameters defined above a value for v close to the electroweak scale $v = 246$ GeV can be obtained.

The complex coupling constant ϵ of the second plaquette term (17) leads to CP violation in the Higgs sector, as evident by the complex vacuum expectation value of the second Higgs doublet in eq. (51). Since it is assumed that $|\epsilon|$ is smaller than $|\kappa|$ by about one order of magnitude, the amount of CP violation is relatively small. Nevertheless, it could lead to potentially important consequences for flavor physics. However, a detailed analysis of CP-violating effects of our model is beyond the scope of this article and is left for future work.

Neglecting the CP-violating contribution from ϵ and m_e^2 , the decomposition of the Higgs doublets into physical states is given by

$$h_a = \begin{pmatrix} \sqrt{2}G^+ \\ v + h^0 + iG^0 \end{pmatrix} \quad h_b = \begin{pmatrix} \sqrt{2}H^+ \\ H^0 + iA^0 \end{pmatrix}. \quad (53)$$

As usual for a 2HDM, one obtains the Goldstone bosons G^0 , G^+ and $G^- = (G^+)^\dagger$, which are eaten by the SM gauge bosons, a neutral pseudoscalar A^0 , a pair of charged scalars H^+ and $H^- = (H^+)^\dagger$, and two CP-even neutral scalars h^0 and H^0 . The pseudoscalar mass is given by $M_A^2 = (m_a^2 + m_b^2)$. The masses of H^\pm and H^0 are very close to M_A , differing only by $\mathcal{O}(m^2/M^2)$ effects.

Including the CP-violating contribution from the m_e^2 parameter would lead to a small mixing between the doublets and between CP eigenstates. However, as mentioned above, these effects will be neglected for the purpose of this work.

The SM-like Higgs boson is h^0 , which at tree-level has a very small mass, in conflict with direct search limits⁴. However, loop corrections to the quartic potential yield positive contributions to m_h . For example, loops involving the top quark and its heavy partners generate a correction of the type

$$\Delta m_h^2 \propto \frac{1}{\pi^2} v^2 \lambda_t^4. \quad (54)$$

In general, these radiative corrections cannot be computed explicitly in the effective little Higgs theory, since they depend on the UV cutoff Λ . However, they are generally comparable

⁴The small tree-level value for m_h is not an artifact of our implementation of X-parity, but would also arise in earlier versions of the minimal moose model in Refs. [1, 2, 4].

Field		X-parity	T-parity	Mass squared
Heavy gauge bosons	$B_{H\mu}^0$	—	—	$\frac{4}{3}g'^2 f^2$
	$W_{H\mu}^0, W_{H\mu}^\pm$	—	—	$4g^2 f^2$
Singlet scalars	η_x	—	—	$4\kappa f^2$
	$\eta_b \equiv \frac{1}{\sqrt{2}}(\eta_y - \eta_z)$	+	—	$(2c_y\lambda_c^2 + c_T\lambda^2)f^2$
	$\eta_a \equiv \frac{1}{\sqrt{2}}(\eta_y + \eta_z)$	+	—	$c_T\lambda^2 f^2$
Triplet scalars	ϕ_x	—	—	$4\kappa f^2$
	$\phi_b \equiv \frac{1}{\sqrt{2}}(\phi_y - \phi_z)$	+	—	$3c_y\lambda_c^2 f^2$
	$\phi_a \equiv \frac{1}{\sqrt{2}}(\phi_y + \phi_z)$	+	—	$m_{g,T}^2 + m_{p,T}^2$
X-odd doublet scalars	h_{H1}	—	+	M_{H1}^2
	h_{H2}	—	+	M_{H2}^2
X-even doublet scalars	H^\pm	+	+	M_A^2
	A^0	+	+	M_A^2
	H^0	+	+	M_A^2
	h^0	+	+	m_h^2
Heavy top partners	T_H	—	—	$4\lambda_c^2 f^2$
	T'	—	—	$4\lambda^2 f^2$
	T	+	+	$4(\lambda^2 + \lambda_c^2)f^2$
Other heavy quarks	Q_H	—	—	$4\lambda_c^2 f^2$
Heavy leptons	L_H	—	—	$4(\lambda_c^l)^2 f^2$

Table 2: List of particles (besides SM particles) below the strong scale Λ and the dominant contributions to their masses. Mass corrections of order $\mathcal{O}(v/f)$ are neglected.

to the electroweak scale and thus could lead to a value of m_h above the current search limit. Since m_h is very sensitive to these loop contributions, we will take it as a free parameters in the following. Note that the loop corrections to the quartic potential have a negligible effect on the masses of the heavy Higgs bosons A^0, H^\pm, H^0 .

4 Phenomenology

In Table 2 the particle content of the model beyond the SM gauge bosons and fermions is summarized. Since the model requires a UV completion, additional degrees of freedom are expected at the scale $\Lambda \sim 10$ TeV, but will not be discussed here.

The charge eigenstates of the gauge bosons and scalars are given by

$$W_H^0 \equiv W_H^3, \quad W_H^\pm \equiv (W_H^1 \mp iW_H^2)/\sqrt{2}, \quad (55)$$

$$\phi_i^0 \equiv \phi_i^3, \quad \phi_i^\pm \equiv (\phi_i^1 \mp i\phi_i^2)/\sqrt{2}. \quad (56)$$

Most new particles have $\mathcal{O}(f) \sim \mathcal{O}(\text{TeV})$ masses. In the table, relative corrections of order $\mathcal{O}(v/f)$ to these mass parameters have been neglected. However, besides the light Higgs boson h^0 , an additional scalar triplet ϕ_a with weak-scale mass is predicted. These scalars are odd under T-parity, so that sizable numbers can be produced only in pairs, but since they are even under X-parity, they can decay through the WZW coupling. In principle, the WZW term also permits single ϕ_a production, but at a highly suppressed rate, which is thus completely negligible. For the same reason, all other T-odd particles will decay first to one of the particles in ϕ_a through T-conserving channels instead of directly decaying via the WZW term.

Since X-parity is exactly preserved, the lightest X-odd particle is stable. If all coupling parameters are not much smaller than unity, the lightest X-odd particle is the heavy U(1) gauge boson, $B_{H\mu}^0$, which is a viable dark matter candidate.

4.1 Electroweak precision constraints

X-parity has been shown to largely reduce the constraints on the parameter space in the case of the littlest Higgs model [4, 16], since corrections to the electroweak precision observables arise only at loop level. Here we calculate the corrections to the electroweak S and T parameters [17] in our model to determine the allowed parameter space.

The dominant contribution to S and T from the fermion sector come from gauge boson self energy diagrams with the X-even T quark running in the loop, a contribution that has already been calculated in Ref. [18]. In spite of the different symmetry structure of the model and the modified implementation of the top-Yukawa couplings the results are almost identical to those obtained in the case of the littlest Higgs model [16]. We find

$$\Delta S = \frac{s_L^2}{2\pi} \left[c_L^2 \left(\frac{(m_T^2 + m_t^2)^2}{(m_T^2 - m_t^2)^2} - \frac{8}{3} \right) + \left(\frac{1}{3} + c_L^2 \frac{2m_t^4 m_T^4 (m_t^2 - 3m_T^2)}{(m_t^2 - m_T^2)^3} - c_L^2 \right) \log \frac{m_t^2}{m_T^2} \right], \quad (57)$$

$$\Delta T = \frac{3}{16\pi} \frac{s_L^2}{c_W^2 s_W^2} \frac{m_t^2}{m_Z^2} \left[s_L^2 \frac{m_T^2}{m_t^2} - 1 - c_L^2 - \frac{2c_L^2}{1 - x_t} \log \frac{m_t^2}{m_T^2} \right], \quad (58)$$

where s_L, c_L are the mixing angles defined in (38) and s_W, c_W are the sine and cosine of the Weinberg angle, respectively. Inserting the leading order expressions for the mixing angles (40) and expanding the expressions in the limit $m_t^2 \ll m_T^2$ one arrives at

$$\Delta S = \frac{1}{2\pi} \frac{\lambda^2}{\lambda_c^2} \frac{m_t^2}{m_T^2} \left(-\frac{5}{3} + \frac{2}{3} \log \frac{m_T^2}{m_t^2} \right), \quad (59)$$

$$\Delta T = \frac{3}{16\pi} \frac{1}{s_W^2 c_W^2} \frac{\lambda^2}{\lambda_c^2} \frac{m_t^4}{m_T^2 m_Z^2} \left(2 \log \frac{m_T^2}{m_t^2} - 2 + \frac{\lambda^2}{\lambda_c^2} \right). \quad (60)$$

Another contribution to the T parameter arises from the custodial symmetry violating mass splitting between the neutral and the charged W_H gauge bosons. At the one loop level this yields [4, 16]:

$$\Delta T_{W_H} = -\frac{9}{16\pi c_W^2 s_W^2 M_Z^2} \Delta M_{W_H}^2 \log \frac{\Lambda^2}{M_{W_H}^2}. \quad (61)$$

The logarithmic divergence forces one to introduce an appropriate counterterm with an unknown coefficient δ_c of order one [4, 16]. In our model the mass splitting is given by

$$\Delta M_{W_H}^2 = \frac{g^2 v^4}{16 f^2} (3 + \sin^2(2\beta) - \cos^2(2\beta)) \approx \frac{g^2 v^4}{8 f^2} \quad (62)$$

Including the counterterm this leads to a contribution to the T parameter of

$$\Delta T_{W_H} = -\frac{1}{4\pi s_W^2} \frac{v^2}{f^2} \left(\delta_c + \frac{9}{4} \log \frac{4\pi}{g} \right). \quad (63)$$

Next we discuss the contributions to electroweak precision observables that arise from the scalar sector. The scalar singlets present in the theory do not contribute to the S and T parameter. Contributions of the scalar triplets to the T parameter are proportional to the mass splitting between the charged and neutral components. This splitting is induced only after electroweak symmetry breaking and is generally small in our model, even for the light X-even triplet.

In the limit of vanishing CP violation in the Higgs sector the contribution of the two X-even Higgs doublets is well approximated by the SM Higgs contribution and the contribution of a heavy Higgs doublet that is given by [19]

$$\Delta T_{2\text{HDM}} = \frac{1}{16\pi s_W^2 c_W^2 m_Z^2} [F(M_{H^+}^2, M_{A^0}^2) + F(M_{H^+}^2, M_{H^0}^2) - F(M_{A^0}^2, M_{H^0}^2)], \quad (64)$$

where

$$F(m_1^2, m_2^2) = \frac{1}{2}(m_1^2 + m_2^2) - \frac{m_1^2 m_2^2}{m_1^2 - m_2^2} \log \frac{m_1^2}{m_2^2}. \quad (65)$$

For small mass differences this contribution is proportional to the mass differences between the charged and neutral heavy Higgs bosons. Since the actual values of $M_{H^\pm}^2 - M_{A^0}^2$ and $M_{H^0}^2 - M_{A^0}^2$ depend on unknown counterterm coefficients and are furthermore sensitive to radiative corrections to the quartic couplings, we take these mass differences as free parameters δ_\pm^2 and δ_0^2 of order $(100 \text{ GeV})^2$. The contribution to the S parameter is small when the mass differences of the heavy scalars are small compared to their masses, so we can neglect it here. Taking into account the CP violation in the Higgs sector only affects the mixing between the Higgs scalars. Since these mixings are small, they do not change the contributions to the S and T parameter significantly.

The X-odd doublets lead to a contribution of similar size, which depends on the incalculable $\mathcal{O}(v^2)$ mass splittings in the h_w and h_x doublets. For simplicity, we do not include

these terms explicitly, since the overall magnitude of the Higgs corrections can be estimated sufficiently well from equation (64).

Other one loop contributions to the T parameter arise from mass splittings in the mirror fermion doublets. The magnitude of such corrections has been estimated in Ref. [16] and it was found that they are suppressed compared to the contributions discussed above.

Apart from the loop-induced contributions to the T parameter the custodial symmetry violating kinetic term of the Goldstone bosons (5) contributes at the tree level through operators of the form⁵

$$\frac{c}{f^2} \left| h_{a,b}^\dagger D_\mu h_{a,b} \right|^2, \quad (66)$$

where $h_{a,b}$ are the X-even Higgs doublets. In our model this leads to a sizable contribution to the T parameter of

$$\Delta T \approx 0.5 \frac{\text{TeV}}{f^2}. \quad (67)$$

This contribution seems to disfavor values of f below about 2 TeV. However, it will be shown below that values of f around 1 TeV can be in agreement with experimental data due to cancellations between different contributions to the T parameter⁶.

The experimental values for the S and T parameters are [20]

$$S = -0.04 \pm 0.09 \quad (68)$$

$$T = 0.02 \pm 0.09 \quad (69)$$

for a Higgs mass of $m_h = 117$ GeV and fixing the U parameter to $U = 0$. The contributions to the S parameter from the top sector are small for all reasonable choices of parameters, and in particular do not lead to additional constraints on regions that give a satisfactory T parameter.

For values of $f > 1$ TeV the contributions of the top sector and the gauge boson sector each stay within the experimental limit of T for most choices of the parameters R and δ_c respectively. The contribution (67), taken separately, would push this value towards $f \gtrsim 2$ TeV. The contribution of the Higgs doublets does not directly constrain the scale f but essentially depends on the mass splitting δ_\pm and δ_0 . When the mass splittings are such that one neutral Higgs is lighter and one heavier than the charged Higgs boson, this contribution is negative and can partially cancel the contribution (67), thus allowing lower values of f . In figure 2 we show that for reasonable choices of the mass splitting parameters and of δ_c these cancellations take place, allowing for values of f at the 1 TeV scale, and even slightly below.

The left plot shows an example where the H^0 is the heaviest Higgs boson and H^\pm is heavier than A^0 , while the right plot shows an example with the hierarchy inverted. For

⁵We thank Ian Low for pointing out the relevance of this operator to us.

⁶Note that a larger custodial symmetry violating contribution from heavy gauge boson exchange in the model of Ref. [2] is forbidden by X- and T-parity.

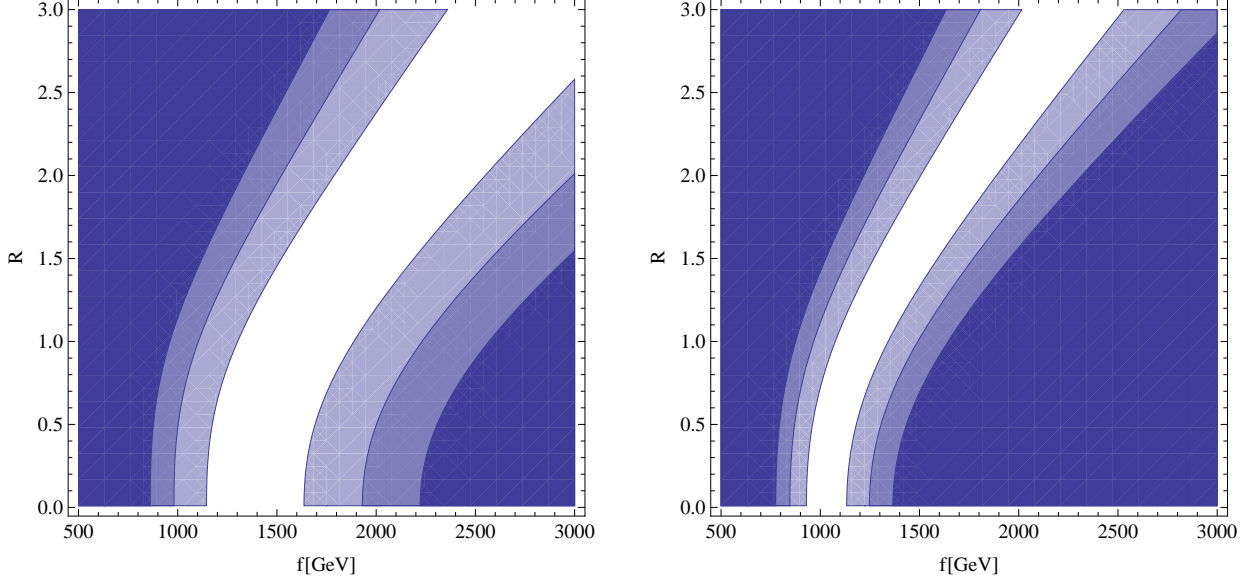


Figure 2: Allowed regions in the f - R parameter space for fixed values of δ_c , δ_{\pm} and δ_0 . From lightest to darkest the shaded regions indicate a deviation of the T parameter from the experimental value by more than one, two and three sigma, respectively. Both plots use $\delta_c = 5$. The mass splittings are $\delta_{\pm}^2 = 0.1f^2$ and $\delta_0^2 = 0.2f^2$ in the left plot and $\delta_{\pm}^2 = -0.15f^2$ and $\delta_0^2 = -0.3f^2$ in the right plot.

both plots the splittings have been chosen proportional to the mass scale f . This causes some regions in the f - R plane to be excluded also for large values of f , since there the contributions from the Higgs loops become dominant.

A moderate amount of fine tuning is involved to cancel the contribution of eq. (67) for smaller values of f . At this point it is worth mentioning that this contribution is absent in models where the Higgs sector has a custodial symmetry, which can be achieved by enlarging the global symmetry group. A concrete realization of this idea, based on a $SO(5) \times SO(5)$ group structure, has been constructed *e. g.* in Ref. [6]. It is certainly possible to extend the present model in a similar way in order to enlarge the allowed parameter space at low scales, however for the sake of simplicity we decided against discussing this here. Furthermore, while this model allows a straightforward ultraviolet completion with QCD-like dynamics, such a construction is less obvious for models that implement a custodial symmetry using orthogonal groups.

4.2 Decays of heavy particles

For concreteness, we assume the plaquette parameter to be close to unity, $\kappa \approx 1$. Furthermore, the UV-sensitive coefficients c_i , introduced below eq. (42), are also assumed to be of order $\mathcal{O}(1)$. As pointed out above, the Yukawa coupling λ_c of the mirror fermions can be chosen relatively large, $\lambda_c \gg 1$, since these fermions do not play any role in compensating the quadratic divergences in the Higgs mass. In this case also the X-even top partner T will

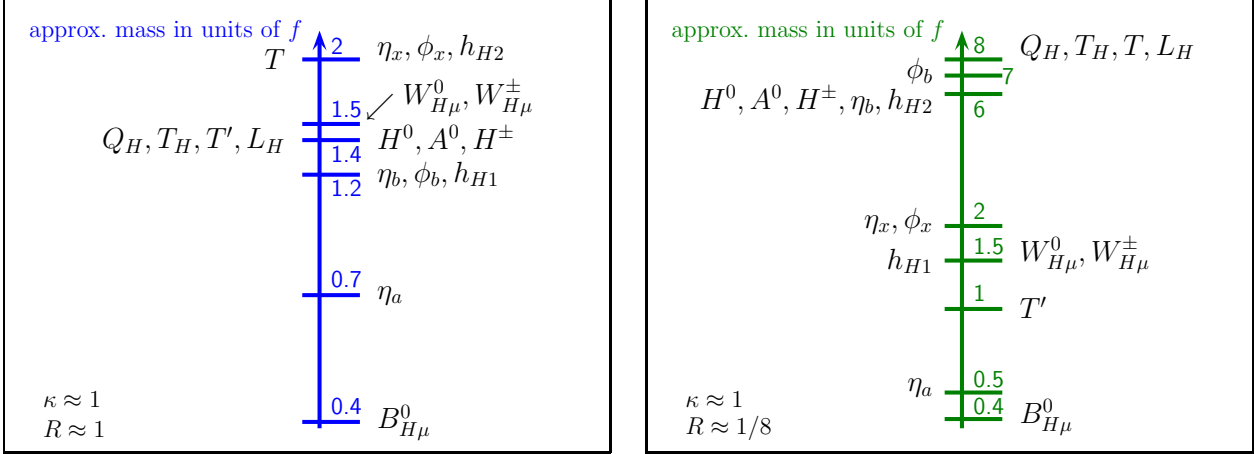


Figure 3: Approximate patterns of two typical spectra of $\mathcal{O}(f)$ particle masses. In both cases, the non-calculable coefficients are assumed to be of order unity, $c_i \approx 1$.

be heavy. As examples, two scenarios will be considered, one with mirror fermion masses near the breaking scale f , and one with very heavy mirror quarks:

$$\text{“Light mirror fermion” scenario:} \quad \lambda_c \approx \lambda \approx 1/\sqrt{2}, \quad R \approx 1, \quad (70)$$

$$\text{“Heavy mirror fermion” scenario:} \quad \lambda_c \approx 4, \quad \lambda \approx 1/2, \quad R \approx 1/8. \quad (71)$$

Note that λ_c , λ and $R = \lambda/\lambda_c$ are related through the top Yukawa coupling (37), which must be $\lambda_t \approx 1/\sqrt{2}$ to reproduce the experimental value for the top-quark mass. The mass hierarchy of the two scenarios is sketched in Fig. 3.

The mass pattern and the conservation of X- and T-parity and gauge symmetries strongly constrain the possible decay channels of the heavy particles. The gauge symmetries, however, are violated by electroweak symmetry breaking, leading to a small mixing between the heavy gauge bosons W_H^0 and B_H^0 , with the mixing angle given by

$$\sin \theta_H = \frac{3gg'}{16(3g^2 - g'^2)} \frac{v^2}{f^2}. \quad (72)$$

While this mixing is suppressed by two powers of v/f , it nevertheless can be relevant for decays of some particles that do not have any other possible decay modes.

The dominant decay channels are summarized in Table 3, for the two scenarios introduced above. Not included in the table are weakly interacting particles with masses larger than about $2f$ and strongly interacting particles with masses larger than about $5f$, since they are expected to be beyond the reach of the LHC (assuming $f \gtrsim 500$ GeV). As mentioned above, the lightest T-odd particle decays through the WZW term, but the WZW contribution is negligible compared to T-conserving interactions for all decays of heavier T-odd particles.

Independent of other parameters, the lightest T-odd particle will be one of the scalars in the triplet ϕ_a , since they do not receive any $\mathcal{O}(f)$ mass terms. At leading order in $1/f$ the WZW term induces decays of into pairs of SM gauge bosons [8]. The masses of the three

“Light mirror fermions” $\kappa \approx 1, R \approx 1$	“Heavy mirror fermions” $\kappa \approx 1, R \approx 0.09$
$Q_H \rightarrow q B_H^0; \quad L_H \rightarrow l B_H^0$ $T' \rightarrow t B_H^0$ $T \rightarrow t h^0, t H^0, t A^0, b H^+, T' B_H^0$	$T' \rightarrow t B_H^0$
$W_H^0 \rightarrow \bar{f} F_H, f \bar{F}_H$ $W_H^\pm \rightarrow \bar{f}' F_H, f' \bar{F}_H$	$W_H^0 \rightarrow h^0 B_H^0$ $W_H^\pm \rightarrow W^\pm B_H^0$
$H^0 \rightarrow t\bar{t}$ $A^0 \rightarrow t\bar{t}; \quad H^+ \rightarrow t\bar{b}$	
$h_{H1}^{0,\pm} \rightarrow t\bar{t} \phi_a^{0,\pm} B_H^0$	$h_{H1}^{0,\pm} \rightarrow t \bar{T}' \phi_a^{0,\pm}, \bar{t} T' \phi_a^{0,\pm}$
$\eta_a \rightarrow h^0 \phi_a^0$ $\phi_a^0 \rightarrow W^+ W^-, Z^0 Z^0, Z^0 \gamma, \gamma \gamma$ $\phi_a^\pm \rightarrow (W^\pm)^* \phi_a^0, W^\pm Z, W^\pm \gamma$	$\eta_a \rightarrow h^0 \phi_a^0$ $\phi_a^0 \rightarrow W^+ W^-, Z^0 Z^0, Z^0 \gamma, \gamma \gamma$ $\phi_a^\pm \rightarrow (W^\pm)^* \phi_a^0, W^\pm Z, W^\pm \gamma$
$\eta_b \rightarrow (A^0)^* \phi_a^0, (H^\pm)^* \phi_a^\mp, (A^0)^* \eta_a$ $\phi_b^0 \rightarrow (A^0)^* \phi_a^0, (H^\pm)^* \phi_a^\mp, (A^0)^* n_a$ $\phi_b^\pm \rightarrow h^0 \phi_a^\pm$	

Table 3: Dominant decay modes for heavy particles expected to be observable at the LHC, for the two qualitative spectra in Fig. 3. Weakly interacting particles with masses $M \gtrsim 2f$ and strongly interacting particles with masses $M \gtrsim 5f$ are not listed, since they are assumed to be beyond the reach of the LHC. $(X)^*$ indicates an off-shell particle.

scalars $\phi_a^{0,\pm}$ are almost degenerate, with a small splitting between the neutral ϕ_a^0 and the charged ϕ_a^\pm incurred from EWSB and the gauge boson loop contribution $m_{g,T}$ in eq. (42) only at order $\mathcal{O}[g^4 f^2/(4\pi^2)] \sim \mathcal{O}[g^4 v^2]$. At this order, higher-order operators from the UV completion could yield additional contributions to the mass splitting, so that it cannot be calculated reliably from the effective little Higgs model. For concreteness, we will therefore assume that the ϕ_a^\pm are slightly heavier than ϕ_a^0 , opening up the decay $\phi_a^\pm \rightarrow (W^\pm)^* \phi_a^0$ through a virtual W boson. Depending on the magnitude of the mass splitting, this decay could dominate over the direct decays into $W^\pm \gamma$ and $W^\pm Z$ that are mediated by the WZW term.

In the “light mirror fermion” scenario, since the SU(2) gauge bosons $W_H^{0,\pm}$ are relatively heavy, they can decay into a mirror fermion plus the corresponding SM partner fermion. Decays of $W_H^{0,\pm}$ directly to the lightest X-odd particle B_H^0 via emission of SM gauge bosons or Higgs bosons are suppressed by $\mathcal{O}(v^2/f^2)$. Therefore, these channels have a branching ratio of at most a few per-cent. Similarly, to leading order in v/f , the other two top partners T and T' are SU(2) singlets and thus only interact through Yukawa or U(1) couplings. Consequently, they do not contribute significantly to heavy SU(2) gauge boson decays.

The X-odd fermions can only decay to the heavy hypercharge boson B_H^0 . Although the

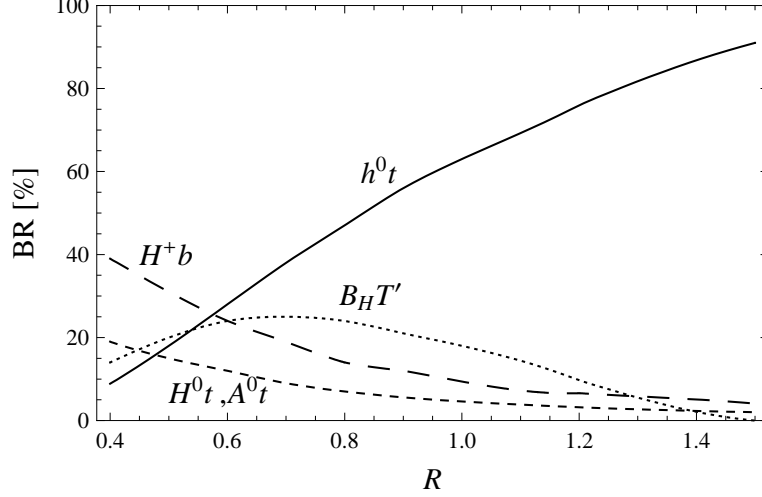


Figure 4: Branching fractions for the dominant decay modes of the X-even T quark, as a function of $R = \lambda/\lambda_c$, and for $f = 1$ TeV.

mirror fermions are not charged under the heavy hypercharge group (see Table 1), this decay is enabled through the mixing between W_H^0 and B_H^0 .

The situation is different for the X-even T quark, which has sizable couplings to the Higgs bosons from the top Yukawa term (34) and to the B_H^0 boson via its hypercharge quantum number. Figure 4 shows the branching fractions for the dominant decay modes as a function of the Yukawa coupling ratio R . For the purpose of this plot, the Higgs boson masses have been calculated using the loop-induced mass terms from section 3.2 with $c_i = 1$. The branching ratios depend only mildly on f . As evident from the plot, the decay $T \rightarrow h^0 t$ is dominant in most of the parameter space, but decays into the heavier Higgs boson can become sizable.

In the second scenario, the mirror fermions and many scalar particles are too heavy to be observables at the LHC. In this case, the gauge bosons $W_H^{0,\pm}$ decay to the B_H^0 via emission of a SM gauge boson or the little Higgs boson. As mentioned above, the T' top partner, which is always lighter than the heavy SU(2) gauge bosons, is a SU(2) singlet. As a result, the decay $W_H^+ \rightarrow T' \bar{b}$ is forbidden, while the channel $W_H^0 \rightarrow T' \bar{t}, \bar{T}' t$ can only proceed through the small mixing of the W_H^0 with the B_H^0 . Therefore this leads to an additional suppression compared to the decay $W_H^0 \rightarrow h^0 B_H^0$:

$$\Gamma[W_H^0 \rightarrow T' \bar{t}, \bar{T}' t] \propto \cos^2 \theta_H \approx 10^{-3} \times v^4/f^4, \quad \Gamma[W_H^0 \rightarrow h^0 B_H^0] \propto v^2/f^2. \quad (73)$$

Consequently, the decay of the heavy SU(2) gauge bosons into the top partner T' can be neglected.

The X-even Higgs bosons H^0 , A^0 , and H^\pm decay predominantly into third-generation SM fermions through the Yukawa couplings eqs. (22),(27). On the other hand, their coupling to the SM gauge bosons is suppressed by the small mixing angle β , see eq. 52, rendering these decay channels negligible.

Of the X-odd doublet scalars, one doublet is typically very heavy. The lighter doublet

h_{H1} contains one CP-even and one CP-odd neutral scalar and two charged states. Their decays are strongly constrained by their charges under X- and T-parity. If the T' is light enough, three-body decay channels are open, otherwise the scalars in h_{H1} can only decay into a four-body final state.

For the singlet scalars the plaquette operator (16) is the only interaction term in the model. At tree-level, the η_b singlet can decay into $A^0 \phi_a^0$, $H^\pm \phi_a^\mp$, and $A^0 \eta_a$, which all have partial widths of the roughly the same order. As the masses of η_b , A^0 and H^\pm are close to each other, the doublet Higgs bosons must be slightly off-shell in these decays. In the same way one obtains the decay modes of $\phi_b^{0,\pm}$.

4.3 Collider phenomenology

For values of f near 1 TeV, several of the new particles predicted by the minimal moose model with exact X-parity are within reach of the LHC. We have calculated cross sections using the program COMPHEP 4.4 [21], using a model file generated with the help of the LAMHEP package [22].

The production of heavy gauge bosons ($W_{\text{H}}^{0,\pm}$) and mirror quarks (Q_{H}) proceeds in the same way as for the littlest Higgs model with T-parity, since all relevant interactions are constrained by gauge invariance. The reader is referred to the literature on the littlest Higgs model for more details on production channels and cross sections [23]. However, compared to the littlest Higgs model, the X-odd gauge bosons are heavier in the minimal moose model (as a function of f). As a result, production cross section for these heavy gauge bosons are relatively small throughout the allowed parameter range.

A special feature of our model are the light triplet scalars $\phi_a^{0,\pm}$. Since they are odd under T-parity, the single production cross section is negligible, but pair production can lead to sizable rates. The lightest T-odd scalar, assumed to be the ϕ_a^0 , decays through the WZW interaction into two SM gauge bosons. In particular, the decay into two photons is allowed, leading to striking signatures with one charged lepton or jet and up to four photons in the final state.

The main production mode for ϕ_a pairs at the LHC are the Drell-Yan processes with the Feynman diagrams shown at the left of Fig. 5. The tree-level cross sections are also shown in Fig. 5. The production of ϕ_a pairs from gluon fusion through s-channel Higgs boson exchange is suppressed by several powers of v/f . We have checked explicitly that this channel is negligible compared to the leading Drell-Yan mode. $W^\pm + 3\gamma$ and $W^\pm + 4\gamma$ are the most exciting final states that result from ϕ_a pair production.

For all other exotic scalars in the model the productions cross sections are small, $\mathcal{O}(\text{fb})$ or below, since those particles are relatively heavy and have only couplings of weak interaction strength. Therefore the observation of any of these scalars from direct production at the LHC would be very challenging.

On the other hand, colored particles have relatively large cross sections at the LHC, in particular the top-quark partners T , which can be produced singly, and T' , which is predicted to be relatively light to cancel the quadratic divergences to the Higgs mass parameter.

Single T production, $pp \rightarrow T\bar{b} + X$, $\bar{T}b + X$ proceeds dominantly through the partonic

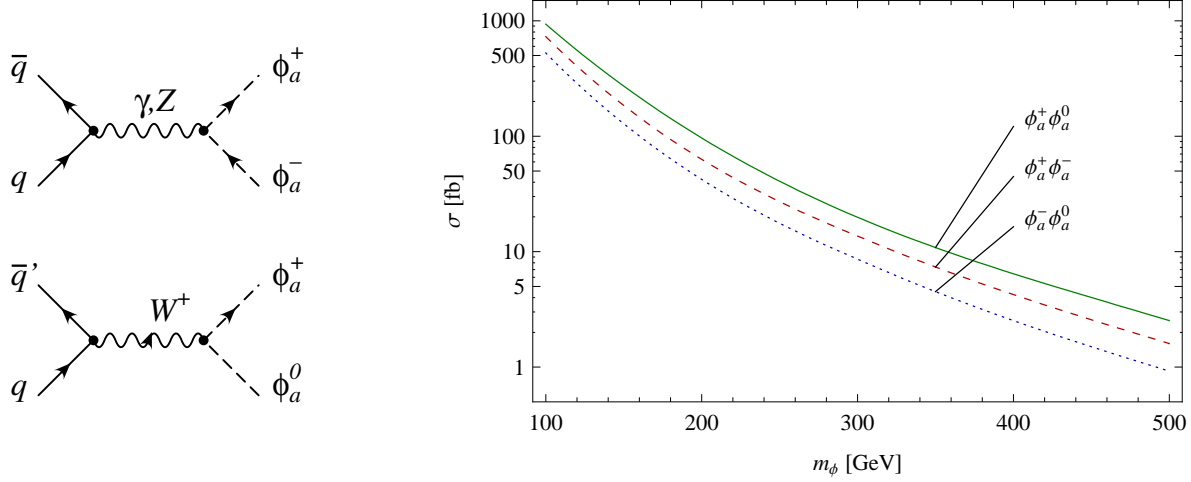


Figure 5: Pair production diagrams and LHC cross sections for the particles in the lightest scalar triplet, as a function of their mass. The factorization scale has been set to m_ϕ , and the center-of-mass energy is $\sqrt{s} = 14$ TeV.

processes $b\bar{q} \rightarrow T\bar{q}'$ and $\bar{b}q \rightarrow \bar{T}q'$, where q, q' are SM quarks of the first two generations. The initial-state bottom quarks can be thought of originating from gluon splitting, $g \rightarrow b\bar{b}$, but for the purpose of this analysis we use the alternative formulation where the bottom quarks are included in the parton distribution functions, see for example Ref. [24]. T quarks can also be produced in pairs through the partonic processes $gg \rightarrow T\bar{T}$ and $q\bar{q} \rightarrow T\bar{T}$. The LHC production cross sections are shown in Fig. 6 (a).

Single T production is mediated mainly by t-channel exchange of W bosons, which couple only to the small top-quark admixture in T , see eq. (40). As a result, the single T cross section strongly depends on the mixing parameters, and thus on $R = \lambda/\lambda_c$. In contrast, the pair production process is mainly governed by QCD gluon exchange and thus insensitive to mixing. In spite of the coupling suppression of the single T contribution this process is dominant for $M_T \gtrsim 1$ TeV, owing to the smaller mass of the final state system (see Fig. 6 (a)).

For relatively low values of M_T , the production rates can reach several tens of fb. The dominant decay mode $T \rightarrow h^0 t$ leads to the signature $4b + W$ in the single T mode if the little Higgs is light, $m_{h^0} \lesssim 130$ GeV, and thus mainly decays via $h^0 \rightarrow b\bar{b}$. The separation of this signal from the SM background is challenging and requires a dedicated analysis.

Figure 6 (b) shows the pair production cross section for T' quarks. Since it is quite possible that the $M_{T'} < 1$ TeV, the cross section can amount to several 100 fb. However, the decay $T'\bar{T}' \rightarrow t\bar{t} B_H^0 B_H^0$ leads to a signature that is very similar to SM $t\bar{t}$ production and requires a careful analysis to disentangle from this background [23, 25].

Besides new particle production, SM processes can be modified by the effect of virtual heavy particle contributions. In particular, the production rate of the SM-like light Higgs boson h^0 via gluon fusion can receive sizable corrections from loop diagrams involving the heavy top partners. However, this effect is not unique to our implementation of X-parity, but it is completely analogous to the littlest Higgs model, described in detail in Ref. [26].

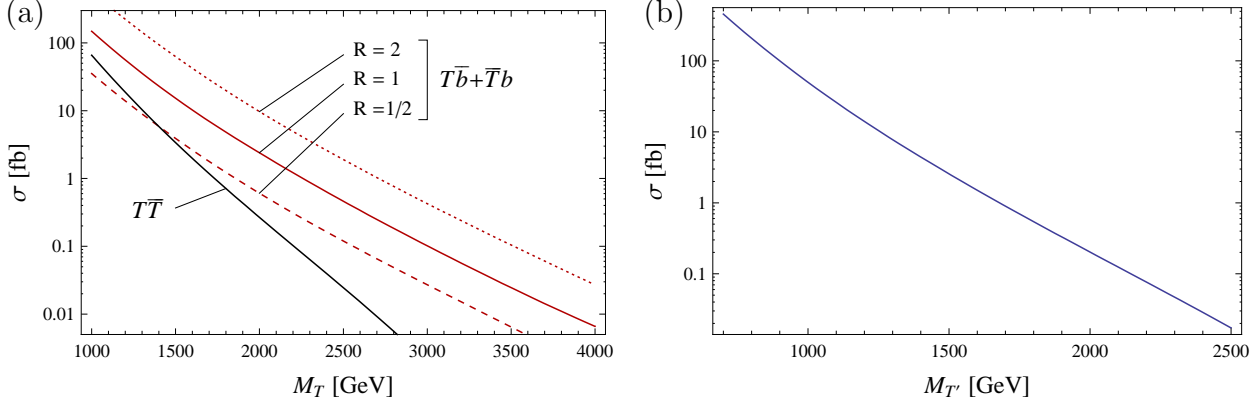


Figure 6: (a) LHC cross sections for single T and $T\bar{T}$ production, as a function of the T quark mass, and for different values of $R \equiv \lambda/\lambda_c$. (b) LHC cross section for $T'T'$ production, as a function of the T' mass. In each plot, the QCD and factorization scales have been set to $M_{T(\prime)}$, and the center-of-mass energy is $\sqrt{s} = 14$ TeV.

5 Summary

In this paper we present a little Higgs model where a new X-parity is implemented such that it is not broken by operators that are typically introduced in strongly coupled ultraviolet completions. This symmetry can therefore be exact up to very high scales and in particular reestablishes the lightest X-odd particle as a viable Dark Matter candidate for little Higgs models.

Our construction is based on the Minimal Moose little Higgs model. Following [11] we introduce X-parity as an exchange symmetry between the link fields in the model. The gauge transformation properties of the link fields are chosen such that the gauged WZW term is even under X-parity while ensuring that the additional heavy gauge bosons present in the model remain X-odd. An additional approximate \mathbb{Z}_2 symmetry further restricts the interactions in the scalar sector and removes potentially dangerous operators. In the fermion sector a set of mirror-fermions is introduced in order to implement X-parity without generating large four fermion operators. An additional pair of top quark partners is introduced to avoid large breaking of the global symmetry that protects the Higgs mass. Mass terms for the mirror fermions and the additional top quark are introduced in a X-invariant way while preserving enough global symmetries to not generate a large mass for the Higgs fields.

Below the symmetry breaking scale f , a light X-even Higgs boson and a scalar triplet ϕ_a remains in the spectrum of the model. In addition, the masses of the B_H gauge boson and of the scalar singlet η_a are parametrically smaller than f . For all reasonable choices of parameters the B_H is the lightest X-odd particle and therefore the Dark Matter candidate, similar to the original little Higgs models with X-parity. The Higgs sector has the structure of a two-Higgs doublet model with one heavy doublet. Successful electroweak symmetry breaking is achieved with moderate fine tuning of parameters and yields a light physical Higgs boson. The model includes a number of additional scalars, which do not acquire vacuum expectation values since they are odd under one of the two parities. Most of these

scalars obtain large $\mathcal{O}(f)$ masses, except for the aforementioned ϕ_a , which has a mass of order the electroweak scale.

The contributions to the electroweak S and T parameters from our model are moderate, allowing for new physics scales as low as $f \sim 1$ TeV. This opens the possibility for the model to be detectable at the LHC within the first years of running. In addition to the usual decay signatures of little Higgs models, the light scalar triplet can be pair-produced copiously at hadron colliders and yields a peculiar signature from its main decay channels into photons or W and Z boson pairs. Probing the top quark sector of the model is more challenging since most signatures suffer from a large standard model background. It would be interesting to study the phenomenological signatures of this model in more detail, in particular whether it can be distinguished from other little Higgs models. Also the question whether the B_H can account for the observed dark matter density in the universe remains to be answered.

Our model is a realistic realization of the little Higgs mechanism with dark matter. More elaborate constructions can be envisaged where the parameter space is less constrained by low energy bounds.

Acknowledgements

The authors would like to thank H.-C. Cheng, A. von Manteuffel and in particular I. Low for useful discussions. This project was supported in part by the Schweizer Nationalfonds.

References

- [1] N. Arkani-Hamed, A. G. Cohen, E. Katz, A. E. Nelson, T. Gregoire and J. G. Wacker, JHEP **0208**, 021 (2002).
- [2] C. Kilic and R. Mahbubani, JHEP **0407**, 013 (2004).
- [3] H. C. Cheng and I. Low, JHEP **0309**, 051 (2003).
- [4] H. C. Cheng and I. Low, JHEP **0408**, 061 (2004).
- [5] N. Arkani-Hamed, A. G. Cohen, T. Gregoire and J. G. Wacker, JHEP **0208**, 020 (2002).
- [6] S. Chang and J. G. Wacker, Phys. Rev. D **69**, 035002 (2004);
A. Birkedal-Hansen and J. G. Wacker, Phys. Rev. D **69**, 065022 (2004).
- [7] C. Csaki, J. Heinonen, M. Perelstein and C. Spethmann, arXiv:0804.0622 [hep-ph].
- [8] J. Wess and B. Zumino, Phys. Lett. B **37**, 95 (1971);
E. Witten, Nucl. Phys. B **223**, 422 (1983);
O. Kaymakalan, S. Rajeev and J. Schechter, Phys. Rev. D **30**, 594 (1984).
- [9] C. T. Hill and R. J. Hill, Phys. Rev. D **75**, 115009 (2007);
C. T. Hill and R. J. Hill, Phys. Rev. D **76**, 115014 (2007).

- [10] V. Barger, W. Y. Keung and Y. Gao, Phys. Lett. B **655**, 228 (2007);
A. Freitas, P. Schwaller and D. Wyler, JHEP **0809**, 013 (2008).
- [11] D. Krohn and I. Yavin, JHEP **0806**, 092 (2008).
- [12] I. Low, JHEP **0410**, 067 (2004).
- [13] H. C. Cheng, I. Low and L. T. Wang, Phys. Rev. D **74**, 055001 (2006).
- [14] M. Blanke, A. J. Buras, A. Poschenrieder, S. Recksiegel, C. Tarantino, S. Uhlig and A. Weiler, JHEP **0701**, 066 (2007).
- [15] S. R. Coleman, J. Wess and B. Zumino, Phys. Rev. **177**, 2239 (1969);
C. G. Callan, S. R. Coleman, J. Wess and B. Zumino, Phys. Rev. **177**, 2247 (1969).
- [16] J. Hubisz, P. Meade, A. Noble and M. Perelstein, JHEP **0601**, 135 (2006).
- [17] M. E. Peskin and T. Takeuchi, Phys. Rev. D **46** 381, (1992).
- [18] L. Lavoura and J. P. Silva, Phys. Rev. D **47** 2046, (1993).
- [19] J. F. Gunion, H. E. Haber, G. L. Kane and S. Dawson, *The Higgs Hunter's Guide*, (Basic Books, New York, 1990).
- [20] C. Amsler *et al.* [Particle Data Group], Phys. Lett. B **667** (2008) 1.
- [21] E. Boos *et al.* [CompHEP Collaboration], Nucl. Instrum. Meth. A **534**, 250 (2004).
- [22] A. Semenov, Comput. Phys. Commun. **180**, 431 (2009).
- [23] J. Hubisz and P. Meade, Phys. Rev. D **71**, 035016 (2005);
A. Freitas and D. Wyler, JHEP **0611**, 061 (2006);
A. Belyaev, C. R. Chen, K. Tobe and C. P. Yuan, Phys. Rev. D **74**, 115020 (2006);
M. S. Carena, J. Hubisz, M. Perelstein and P. Verdier, Phys. Rev. D **75**, 091701 (2007);
D. Choudhury and D. K. Ghosh, JHEP **0708**, 084 (2007).
- [24] J. M. Campbell *et al.*, contributed to the *3rd Les Houches Workshop: Physics at TeV Colliders, Les Houches, France, 26 May – 6 Jun 2003* [arXiv:hep-ph/0405302];
W. K. Tung, in *Proceedings of the Workshop on Physics Simulations at High Energy, Madison, Wisconsin, 1986*, ed. V. Barger *et al.* (World Scientific, Singapore, 1986), pp. 601–613.
- [25] T. Han, R. Mahbubani, D. G. E. Walker and L. T. E. Wang, JHEP **0905**, 117 (2009).
- [26] C. R. Chen, K. Tobe and C. P. Yuan, Phys. Lett. B **640**, 263 (2006).